Role of Bv8 in neutrophil-dependent angiogenesis in a transgenic model of cancer progression

Farbod Shojaei, Mallika Singh, Jennifer D. Thompson, and Napoleone Ferrara*

Genentech, Inc., 1 DNA Way, South San Francisco, CA 94080

Contributed by Napoleone Ferrara, December 24, 2007 (sent for review November 21, 2007)

The secreted Bv8 protein has been recently characterized as a regulator of myeloid cell mobilization and a neutrophil-derived mediator of tumor angiogenesis in several xenografts, but its role in tumor progression in an endogenous setting was unknown. The rat insulin promoter (RIP)–T-antigen (Tag) is a well characterized transgenic mouse model of multistage pancreatic β-cell tumorigenesis. Also, the role of neutrophils in RIP-Tag angiogenic switching, as assessed by systemic ablation using anti-Gr1 antibodies at different stages of tumor progression, has been recently described. Here, we show that early treatment of RIP-Tag mice with anti-Bv8 antibodies resulted in a significant reduction in the number of angiogenic islets relative to control antibody-treated mice, implicating Bv8 in the angiogenic switch during neoplasia. Histological analysis showed a significant reduction in vascular surface areas in hyperplastic and angiogenic lesions in pancreatic islets from anti-Bv8-treated mice. Anti-Bv8 treatment also inhibited the mobilization and homing of CD11b+Gr1+ cells to the peripheral blood and the emerging neoplastic lesions. However, anti-Bv8 treatment had no effect on tumor vascularization or burden when initiated at later stages of tumor progression. The stage-dependent efficacy of anti-Bv8 treatment appears remarkably similar to that reported after neutrophil ablation, suggesting that Bv8 is an important mediator of neutrophil-dependent angiogenesis in this transgenic model. In summary, our studies verify a role for Bv8 in the mobilization and recruitment of myeloid cells and in the induction of tumor angiogenesis in the early stages of neoplastic progression.

prokineticin | tumor | myeloid cell | VEGF

It is now well established that angiogenesis plays a crucial role in tumor progression (1). Vascular endothelial growth factor (VEGF)-A is one of the most important regulators of physiological and/or pathological angiogenesis (2). Loss of a single allele of the VEGF-A gene results in embryonic lethality in mice (3). Several VEGF inhibitors have been approved by the Food and Drug Administration for the treatment of advanced malignancies and age-related macular degeneration (4, 5). Although tumor cells have been long considered to be the main source of VEGF and other angiogenic factors, much recent work has emphasized the role of inflammatory cells in different aspects of tumorigenesis (reviewed in ref. 6). Recent studies suggest that factors selectively expressed by subsets of inflammatory cells may regulate tumor angiogenesis (7).

Rat insulin promoter (RIP)–T-antigen (Tag) mice represent a transgenic model of insulinoma driven by the expression of simian virus 40 Tag oncoproteins under the control of RIP, resulting in a well defined multistage tumor progression (8). Histopathological studies have revealed three distinct stages in tumor development and progression in this model initiated with hyperplastic lesions (≈5 weeks of age) followed by the development of angiogenic islets (≈7 weeks of age). A fraction of angiogenic islets progress to carcinomas at ≈12–14 weeks of age, and the mice typically succumb to a combination of tumor burden and hyperinsulinemia by ≈16 weeks.

The predictable tumor development in the RIP-Tag model allows preclinical testing of therapeutic agents at different stages of tumor progression. In particular, therapeutic intervals defined as "prevention" (5–10 weeks of age), "intervention" (10–13 weeks of age), and "regression" (12–14 weeks of age) have been described (9), allowing investigation of the effects of therapy in tumor initiation, malignant conversion, and late-stage tumorigenesis, respectively. Early studies suggested a crucial role for VEGF-A in each stage of tumor development in RIP-Tag mice (10). Conditional deletion of VEGF-A in pancreatic cells resulted in a significant reduction in angiogenic switching and consequently, the number of angiogenic islets. Moreover, the RIP-Cre; $VEGF^{fl/fl}$; RIP-Tag mice showed a dramatic reduction in the number of tumors and consequent tumor burden in the carcinoma stages (10).

Recently, Nozawa *et al.* (11) showed that infiltrating neutrophils, identified as Gr1+ cells, are an important cell type in the initial angiogenic switch in RIP-Tag mice as a source of matrix metalloproteinase type 9, which in turn affects the bioavailability of VEGF-A for VEGFR2. However, the role (if any) of angiogenic factors other than VEGF in neutrophil-mediated angiogenic switching in RIP-Tag mice remained to be determined.

EG-VEGF and Bv8 are two highly related secreted proteins, also referred to as prokineticin-1 and prokineticin-2, which belong to a larger class of peptides defined by a five-disulphide bridge motif called a colipase fold (12–16). Both bind two highly homologous G protein-coupled receptors EG-VEGRF/PKR-1 and EG-VEGFR/PKR-2 (17, 18). Bv8 was isolated and cloned from the skin of the frog *Bombina variegata* (19) and was found to induce gastrointestinal motility and hyperalgesia, similar to the homologous MIT-1 protein, previously purified from the venom of the black mamba snake (20, 21). Later on, the human orthologues of these two highly conserved proteins were shown to have the same motility-enhancing activity as the nonmammalian proteins (13). More recently, several important functions have been associated with Bv8 receptor signaling, including regulation of circadian rhythms (22), olfactory bulb neurogenesis, and survival of GnRH neurons (23, 24). Interestingly, mutations in the genes encoding Bv8 or PKR-2 have been associated with Kallman's syndrome (25).

We previously characterized EG-VEGF and Bv8 as mitogens selective for specific endothelial cell types (14, 15, 26, 27). Furthermore, Bv8 or EG-VEGF induced hematopoietic cell mobilization *in vivo* and stimulated production of granulocytic and monocytic colonies *in vitro* (28, 29). We recently reported that Bv8 is a mediator of myeloid cell-dependent tumor angiogenesis in several xenograft models (7). Therapeutically, anti-Bv8 treatment was found to be most efficacious when initiated in the early stages of tumor development (7).

Here, we investigated the role of Bv8 in tumor angiogenesis in RIP-Tag mice using anti-Bv8 mAbs in both prevention and intervention trials, as defined (9). Anti-Bv8 treatment resulted in a significant reduction in the number of angiogenic islets in prevention trials. This effect was associated with a reduction in vascular

Author contributions: F.S. and M.S. contributed equally to this work; F.S., M.S., and N.F. designed research; F.S., M.S., and J.D.T. performed research; F.S., M.S., J.D.T., and N.F. analyzed data; and F.S., M.S., and N.F. wrote the paper.

The authors declare no conflict of interest.

Freely available online through the PNAS open access option.

*To whom correspondence should be addressed. E-mail: ferrara.napoleone@gene.com.

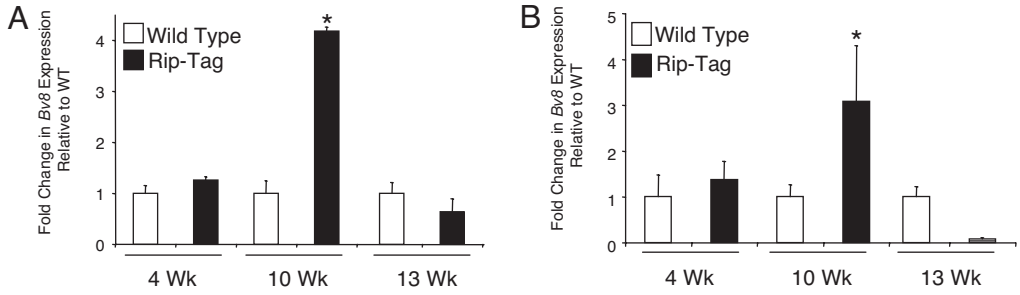

Fig. 1. Bv8 expression in RIP-Tag mice. Total RNA was extracted from BMMNCs (*A*) and pancreata (*B*) of WT, tumor-free (4 weeks old), and tumor-bearing (10 and 13 weeks old) RIP-Tag mice. Bv8 expression was measured by qRT-PCR as described in *Materials and Methods*. Data shown are means ± SEM ($n = 4$). * indicates significant difference by *t* test ($P \leq 0.05$) when comparing Bv8 expression with the corresponding WT group.

surface areas in both hyperplastic and angiogenic lesions and a reduction in tumor-infiltrating CD11b+Gr1+ cells.

Results

Bv8 Is Highly Expressed in Bone Marrow (BM) and Pancreas of RIP-Tag Mice at Early Tumorigenesis Stages. We monitored Bv8 expression in the BM and pancreas at 4 weeks (early stage, hyperplastic islets), 10 weeks (midstage, angiogenic switch), and 13 weeks (late stage, tumors present) of age in RIP-Tag and WT mice. As illustrated in Fig. 1*A* quantitative RT-PCR (qRT-PCR) analysis showed that, whereas *Bv8* is expressed at low level in BM mononuclear cells (BMMNCs) from WT or young (4–5 weeks old) RIP-Tag mice, it is highly expressed in BMMNCs from RIP-Tag mice undergoing angiogenic switching and malignant conversion at 10 weeks of age. However, expression of Bv8 in the BM of 13-week-old RIP-Tag mice was no higher than that in age-matched WT mice. Interestingly, in parallel to the BM, we found a peak in Bv8 expression in the pancreas of 10-week-old RIP-Tag mice (Fig. 1*B*). We also examined the expression of Bv8 receptors, EG-VEGFR1/PKR-1 and EG-VEGFR2/PKR-2, in the BM and pancreas. Although the two receptors were found to be expressed in both tissues, their expression level was not significantly different in early (10 weeks) vs. later (13 weeks) stages of tumorigenesis (data not shown). The relatively high expression of Bv8 at early stages of tumor development, combined with a lack of marked change in receptor expression, is consistent with our previous observations in xenograft models (7).

Anti-Bv8 Treatment Is Efficacious in Prevention but Not in the Intervention Trials in RIP-Tag Mice. The profile of *Bv8* expression during spontaneous neoplastic progression prompted us to assess the role of Bv8 in RIP-Tag tumorigenesis using previously described (7) anti-Bv8 mAbs. Treatment of RIP-Tag mice with anti-Bv8 in prevention trials resulted in a significant reduction in the number of angiogenic islets compared with control mAb-treated animals (Fig. 2*A*). As expected, anti-VEGF treatment also significantly reduced the number of angiogenic islets in the transgenic mice. Morphological analysis of lesions demonstrated multiple areas of hyperemia and hemorrhage, indicative of increase in blood flow and angiogenesis, in control mAb-treated mice compared with anti-Bv8 or anti-VEGF groups (Fig. 2*B*).

In contrast to prevention trials, anti-Bv8 treatment did not result

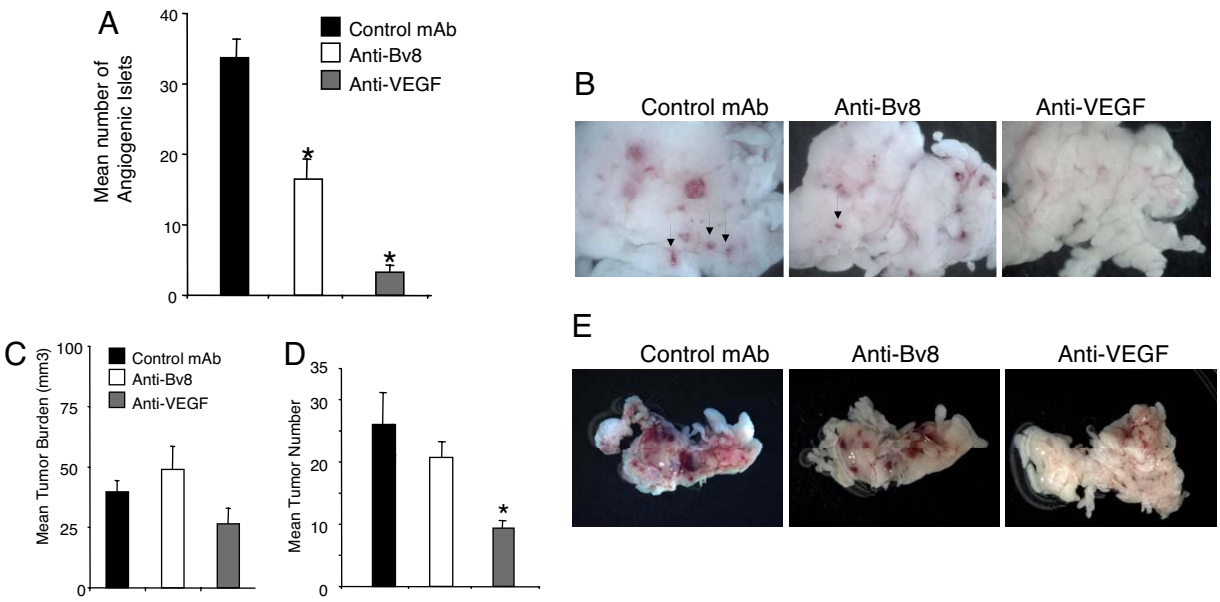

Fig. 2. Bv8 plays a role in tumor angiogenesis in early but not in late stages. (*A*) RIP-Tag mice were treated with control mAb ($n = 12$), anti-Bv8 ($n = 9$), or anti-VEGF ($n = 7$) mAbs for 5 weeks, starting at 5 weeks of age. Angiogenic islets were counted in each treatment group by using a dissection microscope. Bars represent the mean ± SEM of angiogenic islets. (*B*) Representative images from each treatment group, as indicated. Arrows point to the hyperemic lesions. (*C* and *D*) RIP-Tag mice received control mAb ($n = 8$), anti-Bv8 ($n = 6$), or anti-VEGF ($n = 10$) for 3 weeks, starting at 10 weeks of age. Tumor burden (*C*) and number of tumors (*D*) were measured in each treatment group. (*E*) Representative images are shown from each treatment group. Data are representative of two independent experiments, with similar results. * indicates significant difference when compared with control mAb-treated group ($P \leq 0.05$). (Magnification: *B* and *E*, ×0.8.)

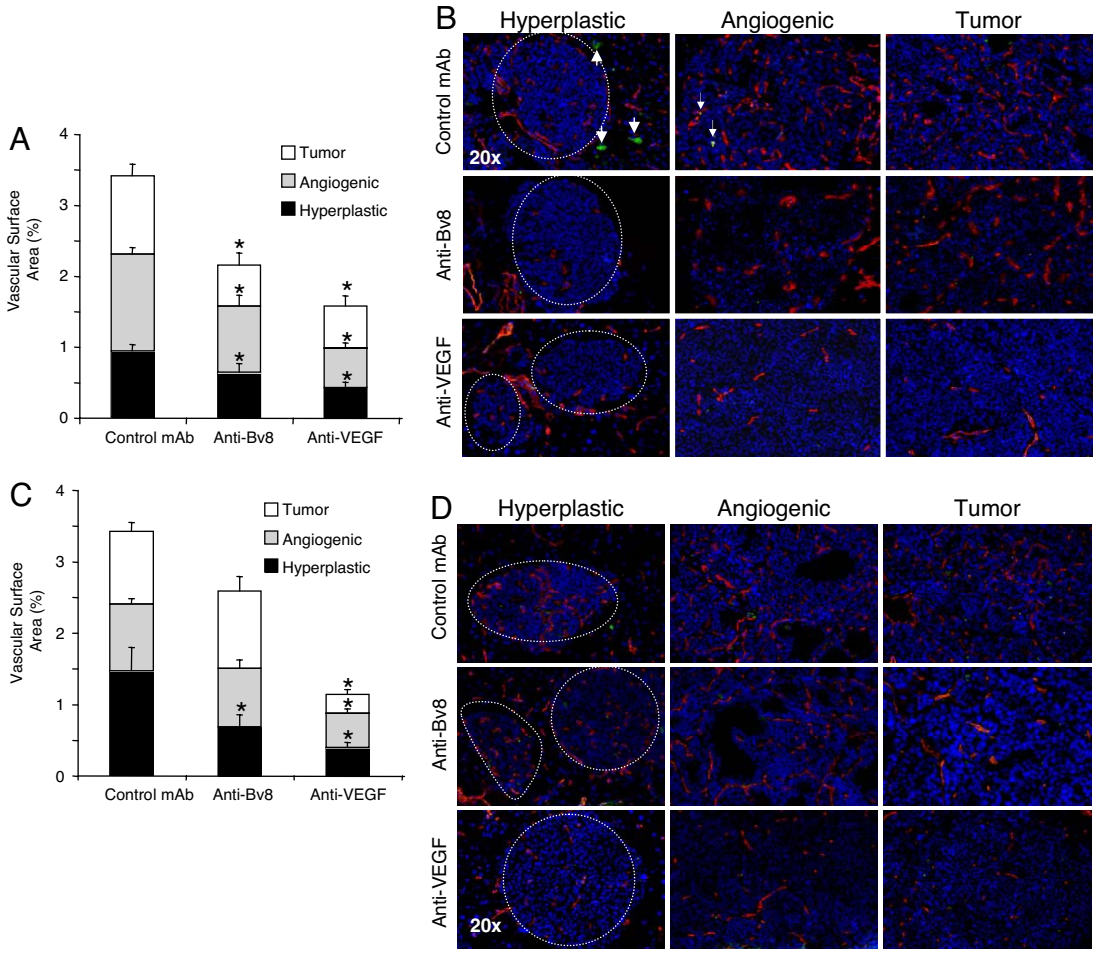

Fig. 3. Anti-Bv8 treatment reduces VSA and neutrophil infiltration in hyperplastic and angiogenic lesions in prevention but not in intervention trials. RIP-Tag mice were treated with control, anti-Bv8, or anti-VEGF mAbs in prevention or intervention trials, as described. Evaluations were performed at the end of such periods. Sections (6 μm) were cut from frozen tumors and stained with anti-CD31 (shown in red) and anti-Gr1 (shown in green) antibodies as described. (*A*) VSA was assessed on the basis of the percentage of CD31+ areas relative to the entire lesion in each treatment group. Bars represent the mean VSA ± SEM. Data represent VSA from at least three mice per treatment. (*B*) Representative images of hyperplastic, angiogenic, and tumor lesions from prevention trials. RIP-Tag mice were treated with control, anti-Bv8, or anti-VEGF mAbs for 5 weeks. Tumor sections were stained with anti-CD31 (shown in red) to label blood vessels and anti-Gr1 (shown in green) to label neutrophils. Nuclear counterstaining with DAPI is shown in blue. Arrows point to Gr1+ cells in hyperplastic and angiogenic lesions. Dotted lines show the boundaries between hyperplastic islets and the surrounding exocrine tissue; angiogenic islet and tumor photomicrographs are focused within the core of the lesion. Anti-Bv8 treatment reduces neutrophil infiltration in the exocrine pancreas. (*C*) RIP-Tag mice were treated in an intervention trial with control, anti-Bv8, or anti-VEGF mAb, and VSA was measured in tumor sections ($n = 3$) as described. (*D*) Images are representative of hyperplastic, angiogenic, and tumor lesions at the end of intervention trials. Vascular structures and neutrophils are shown in red and green, respectively. DAPI-counterstained nuclei are shown in blue. * indicates significant difference ($P \leq 0.05$) when comparision with the control mAb-treated groups. (Magnification: *B* and *D*, ×20.)

in any reduction in tumor burden or tumor size when performed in intervention trials (Fig. 2 *C* and *D*). Anti-VEGF treatment did not affect tumor burden, but it significantly reduced the number of tumors (Fig. 2 *C* and *D*). This observation raises the possibility that, in contrast to intervention trials, tumors at this later stage have a differential response to anti-VEGF therapy such that sensitive tumors are inhibited by the treatment, whereas refractory ones may continue to grow and expand. Microscopic analysis of pancreatic tissues showed fewer areas of hyperemia in tumors from anti-VEGF-treated animals compared with those treated with control or anti-Bv8 mAb (Fig. 2*B*).

Bv8 Plays a Role in the Angiogenic Switch by Affecting the Neoplastic Vasculature and Infiltration of Gr1+ Cells. We stained pancreatic sections from RIP-Tag mice with anti-CD31 and anti-Gr1 antibodies to examine blood vessels and neutrophils at early and later stages of tumor progression. We quantified the vascular surface areas (VSAs) in all identifiable neoplastic lesions from prevention and intervention trials (Fig. 3). We found a significant reduction in the VSAs of hyperplastic and angiogenic lesions from prevention trials in anti-Bv8 and anti-VEGF-treated groups as compared with controls (Fig. 3 *A* and *B*). Pancreata from prevention trials (Fig. 3*B*) showed infiltration of Gr1+ cells into exocrine tissues adjacent to hyperplastic and angiogenic lesions in control mAb- and anti-VEGF-treated mice. Remarkably, pancreata from anti-Bv8-treated mice were essentially devoid of Gr1+ cells (Figs. 3*B* and 4*E*), strongly implicating Bv8 in the homing of neutrophils to the pancreas in RIP-Tag mice.

Anti-Bv8 treatment significantly reduced vascular density in hyperplastic lesions in intervention trials but did not affect the vasculature in angiogenic or adenocarcinoma lesions (Fig. 3 *C* and *D*). This result appears consistent with the hypothesis that Bv8 is primarily implicated in early angiogenic events. In contrast, anti-VEGF showed a potent suppression of the tumor vasculature in all types of pancreatic lesions in the intervention trial setting, consistent with a key role for VEGF in tumor angiogenesis in RIP-Tag

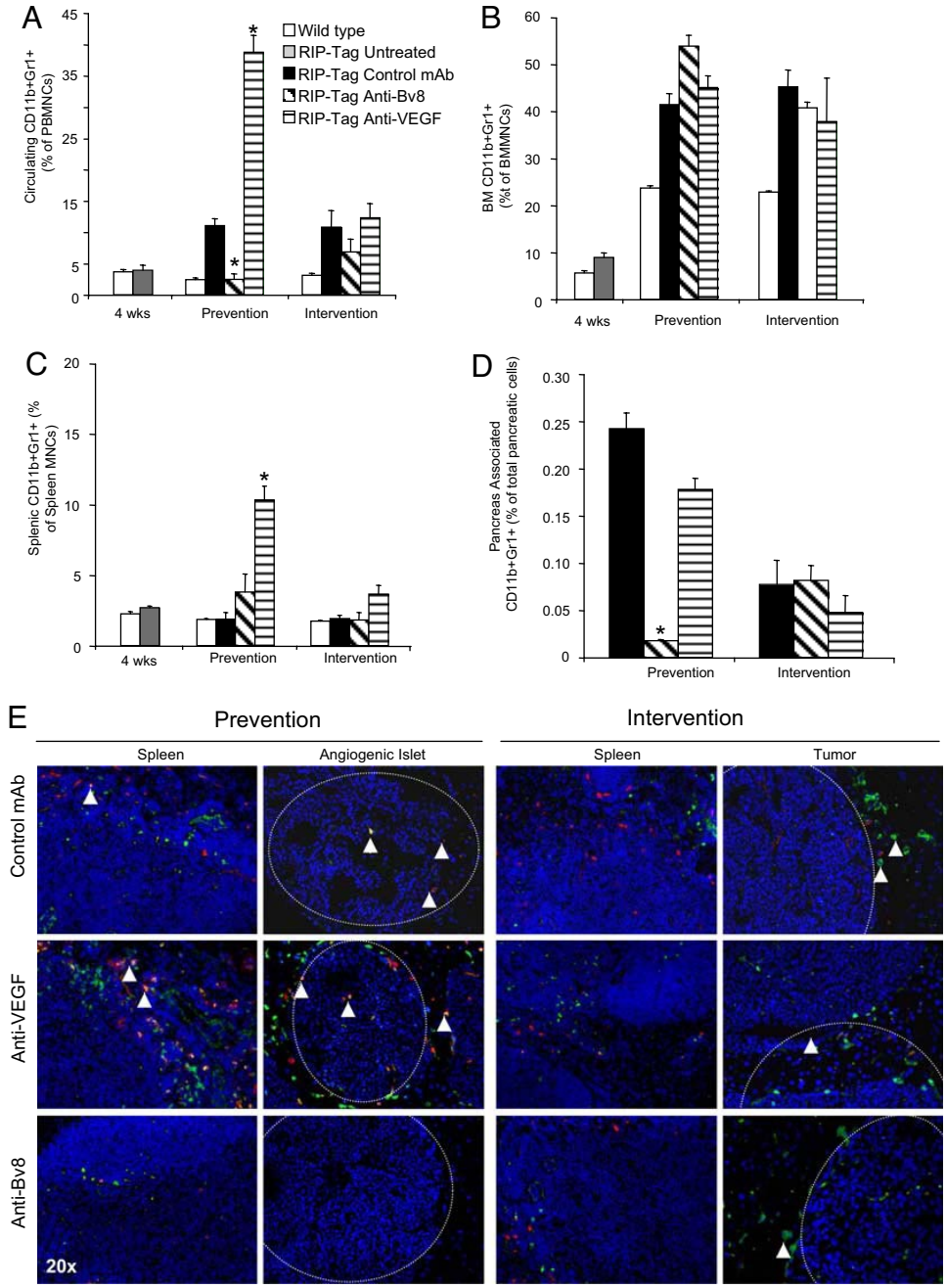

Fig. 4. Anti-Bv8 treatment reduces the frequency of CD11b+Gr1+ cells in PB and pancreas at the end of prevention trials. RIP-Tag mice were treated with control mAb, anti-Bv8, or anti-VEGF, in prevention and intervention trials, as described in *Materials and Methods*. Measurements were performed at the end of such therapeutic intervals. (*A–C*) Mononuclear cells were isolated from PB (*A*), BM (*B*), and spleen (*C*). Cells were stained with fluorochrome-conjugated anti-CD11b and anti-Gr1 antibodies as described in *Materials and Methods*. The frequency of CD11b+Gr1+ cells in each tissue was measured as described. (*D*) Single-cell suspensions were obtained from pancreata and then stained with the same anti-CD11b and anti-Gr1 antibodies as described above. Bar graphs represent the means ± SEM of the frequency of CD11b+Gr1+ cells in each tissue. * indicates significant difference when compared with control mAb-treated group ($P \leq 0.05$). (*E*) Representative images from prevention and intervention trials illustrating immunostaining for CD11b (green) and Gr1 (red) in the spleen, angiogenic islets (prevention) and tumors (intervention) from each treatment cohort. Arrows point to CD11b+Gr1+ cells in and around angiogenic islets and CD11b+ cells in and around tumors. Dotted lines show boundaries between neoplastic lesions and surrounding exocrine tissue. (Magnification: ×20.)

mice (10) (Fig. 3 *C* and *D*). However, analysis of tumor sections in the intervention setting did not reveal any difference in neutrophil infiltration among the treatment groups, further indicating a role for these cells in early but not late stages of tumor progression in RIP-Tag mice (Figs. 3*D* and 4*E*).

Bv8 Regulates Peripheral Mobilization and Homing of CD11b+Gr1+ Cells into Pancreatic Islets Early in Tumor Progression. We examined the kinetics of CD11b+Gr1+ cells in the peripheral blood (PB), BM, spleen, and pancreas of 4-, ≈10- (end of prevention), and ≈13- (end of intervention) week-old RIP-Tag mice by FACS (Fig. 4). Analysis at 10 weeks of age showed a significant ($P \leq 0.05$) reduction in the frequency of circulating CD11b+Gr1+ cells in anti-Bv8 vs. control mAb-treated mice (Fig. 4*A*). Conversely, anti-VEGF treatment increased the mobilization of CD11b+Gr1+ cells to the PB in ≈10-week-old mice. This finding is consistent with previous studies in which long-term treatment with anti-VEGF

antibodies resulted in an increase in the peripheral mobilization of myeloid cells (7). However, neither anti-Bv8 nor anti-VEGF affected circulating CD11b+Gr1+ cells measured at the end of intervention trials. Interestingly, analysis of BM did not show any treatment-induced differences in the frequency of these myeloid cells at ≈10 or ≈13 weeks. Indeed, previous studies in xenograft models indicated that Bv8 primarily affects mobilization of myeloid cells rather than their differentiation within the BM (7). The frequency of CD11b+Gr1+ cells in the spleen did not show any significant change after anti-Bv8 treatment at ≈10 or ≈13 weeks (Fig. 4*C*), whereas anti-VEGF treatment induced an increase in splenic CD11b+Gr1+ cells at ≈10 weeks. The mechanism of such anti-VEGF dependent effects remains to be fully elucidated. Finally, FACS analysis of pancreata documented infiltration of CD11b+Gr1+ cells at ≈10 weeks of age in control mAb- and anti-VEGF-treated mice (Fig. 4*D*). In contrast, anti-Bv8 treatment significantly reduced infiltration of CD11b+Gr1+ cells to the islets.

We then visually confirmed the patterns of CD11b+Gr1+ cell infiltration by immunofluorescent staining for CD11b and Gr1 in spleen and pancreas (Fig. 4*E*). We detected single-positive CD11b and Gr1 cells and double-staining cells in these organs from 10-week-old control mAb-treated mice in prevention trials. In agreement with the report by Nozawa *et al.* (11), we observed Gr1+ neutrophils in and around angiogenic islets at this stage. Consistent with the FACS data (Fig. 4*D*), we also observed CD11b+Gr1+ cells within these lesions and adjacent to germinal centers within the spleen. Anti-VEGF-treated pancreata showed a distinct increase in the infiltration of single- and double-staining cells in both organs, whereas anti-Bv8 treatment showed a distinct reduction in each of these populations. Immunostaining of tumors harvested at the end of intervention trials with these markers revealed a noticeable lack of Gr1+ cells, consistent with a role for neutrophils in angiogenic switching but not at later stages of tumor progression. Interestingly, whereas CD11b+Gr1+ cells were absent in the pancreas and rare in the spleen (as expected from FACS data), we observed an increase in CD11b+ cells in and around the periphery of tumors that was unaffected by either anti-Bv8 or anti-VEGF treatment. The absence of CD11b+Gr1+ cells could explain the lack of response to anti-Bv8 in the intervention trial, because these cells are thought to be the main source of Bv8 (7).

Discussion

Previous studies have suggested a role for myeloid cells in tumor growth and angiogenesis (30, 31). We recently demonstrated that CD11b+Gr1+ myeloid cells are a population mediating refractoriness to anti-VEGF treatment in several tumor models (32). Additionally, we identified the Bv8 protein as an important player of CD11b+Gr1+ cell-mediated tumor angiogenesis (7). Our data in several xenograft models suggested that CD11b+Gr1+ cells isolated from BM, spleen, and tumors are highly enriched sources of Bv8, which regulates mobilization of myeloid cells into the PB and may also promote angiogenesis when locally produced by tumor-infiltrating myeloid cells (7).

To verify the above findings in an immune-competent, spontaneous tumor model, we investigated the role of Bv8 in a genetic model of multistage carcinogenesis. RIP-Tag mice represent a valuable tool for studying the development of the vasculature in different stages of tumorigenesis in nonmalignant and malignant status in pancreatic β-cells (8). Genetic studies have established a key role for VEGF-A in tumor initiation and malignant conversion in this model (10). At later stages, other angiogenic factors such as members of the FGF family have been implicated in mediating resistance to VEGF blockade in RIP-Tag mice (33). Importantly, previous studies defined the contribution of neutrophils, as assessed by systemic ablation using anti-Gr1 antibodies, at different stages of tumor progression in this model (11). These studies demonstrated that, although neutrophils account for only ≈0.4% of the total cell population of angiogenic islets and tumors, ablation of this cell type performed in prevention trials impaired the angiogenic switch, whereas the same treatment had no effect on tumor vascularization and growth when performed in intervention trials (11).

Bv8 expression in BM and tumors exhibited a peak in early tumorigenesis, which is consistent with our previous xenograft studies showing peak concentrations of Bv8 in the BM, tumors, and spleens a few days after tumor implantation (7). In contrast to Bv8, the related EG-VEGF was not expressed in the BM or pancreas of RIP-Tag mice (data not shown), which is in agreement with previous studies showing distinct expression patterns for the two genes in mouse tissues (15, 34).

We previously identified granulocyte colony-stimulating factor (G-CSF) as a key regulator of Bv8 expression (7). In the present study, we found a trend toward higher G-CSF expression in pancreas and BM, overlapping with the changes in Bv8 gene expression (data not shown). However, even small changes in G-CSF level may result in marked increases in Bv8 expression (7). Additional studies with anti-G-CSF antibodies or other inhibitors are required to assess directly the role of G-CSF in regulating Bv8 expression in RIP-Tag mice.

The kinetics of Bv8 expression suggested that anti-Bv8 treatment would be most efficacious in prevention trials. Indeed, we found a significant reduction in the number of angiogenic islets in such trials after anti-Bv8 treatment. The degree of reduction in the number of angiogenic islets (≈50%) was similar to that reported by Nozawa *et al.* (11) by means of systemic neutrophil ablation, implicating Bv8 as an important contributor of neutrophil-dependent angiogenesis in this model.

However, at the end of intervention trials we found no difference in tumor burden or tumor number between anti-Bv8 and control groups. This result is consistent with the relative reduction of Gr1+ cells at later stages of tumor progression and the reported lack of effects of anti-Gr1 treatment in intervention trials (11), albeit we did note an increase in a morphologically distinct CD11b+ cellular population, the role of which remains to be investigated.

To elucidate the mechanism of the antitumor effects of anti-Bv8, we quantified the tumor vasculature and also investigated CD11b+Gr1+ cell infiltration in the tumors. Our data support a role for Bv8 both as a mediator of CD11b+Gr1+ cells mobilization and potentially as a local angiogenic factor. Anti-Bv8 significantly reduced the VSA and also reduced the numbers of angiogenic lesions in prevention trials. Also, immunofluorescent analysis revealed a lack of infiltrating tumor-associated Gr1+ cells in anti-Bv8 treated mice. In fact, the reduction in CD11b+Gr1+ cells in both PB and tumors in RIP-Tag mice after anti-Bv8 treatment was of greater magnitude than that observed in xenografts (7), suggesting that in RIP-Tag mice such effect of anti-Bv8 antibodies may be of greater relevance to their antitumor effects compared with local neutralization of the direct proangiogenic effects of Bv8. Indeed, both FACS and immunofluorescent data indicated a relatively mild infiltration of Gr1+ cells into the tumors, in agreement with other studies examining infiltration of neutrophils and macrophages in the pancreas of RIP-Tag mice (11, 35). These data may indicate that, in contrast to xenografts (7), RIP-Tag islets may contain lower levels of cytokines and chemokines required for chemo-attraction of myeloid cells from the BM to the tumors, particularly at later stages of tumor progression. The much lower frequency of CD11b+Gr1+ cells in the tumors at such a later stage coincides with a lack of response to anti-Bv8 treatment. These data are consistent with the notion that CD11b+Gr1+ cells are the major source of Bv8 during tumor progression in RIP-Tag mice.

We tested the effects of the combination of anti-Bv8 with anti-VEGF treatment in both prevention and intervention trials. We found no evidence of significant additivity (data not shown), possibly reflecting the strong effects of anti-VEGF alone in the intervention trials and the lack of significant contribution of Gr1+ cells to angiogenesis at later stages of tumorigenesis in this model.

Whether administration of cytotoxic agents, resulting in mobilization of neutrophils, may restore a response to anti-Bv8 (7) in an intervention trial, potentially leading to a combinatorial effect, remains to be established.

In conclusion, targeting Bv8 appears to substantially reproduce the consequences of systemic neutrophil ablation in the RIP-Tag spontaneous model of tumorigenesis (11), confirming a role for this cytokine as a mediator of myeloid cell mobilization and myeloid cell-dependent tumor angiogenesis. Further studies are required to dissect molecular mechanisms underlying Bv8 actions and assess the role of this signaling system in additional disease models.

Materials and Methods

Mice. RIP1-Tag2 or RIP-Tag mice have been described (9). In the prevention trials, animals were treated from 5 to ≈10 weeks of age; in the intervention trials, mice were treated from ≈10 to ≈13 weeks of age. All mice were maintained in accordance with the guidelines governing the care of laboratory mice and were killed after their treatment periods.

Antibody Treatments. RIP-Tag mice were treated with anti-Bv8 mAbs 3F1 and 2B9 (each at 5 mg/kg) as described (7) or with anti-VEGF-A mAb G6.23 (36) (2.5 mg/kg) twice a week using an i.p. route of administration. As control, we used isotype-matched anti-Ragweed mAb as reported (7).

qRT-PCR Analysis. Total RNA was extracted from BMMNCs and tumor samples with a Rneasy mini kit (Qiagen) along with on-column DNase-I digestion to exclude genomic DNA contamination. *Taq*man experiments were performed in an optical 96-well reaction plate and on a 9600 Emulation mode of 7500 real-time PCR machine (Applied Biosystems) using protocols provided by the manufacturer. We used 100 ng of the total RNA per reaction. The expression level of each gene was quantified against GAPDH, as the housekeeping gene, in the same treatment as described (7). PCR conditions comprised of incubations of 30 min at 48°C, 10 min at 95°C, and 40 cycles of 15 s at 95°C and 60 s at 60°C. Oligonucleotide sequences for Bv8 and GAPDH have been described (7).

Flow Cytometry. BMMNCs were isolated by flushing the femur and tibia of all of the treated mice with plain DMEM. Whole blood was isolated by using vacutainers (BD) containing EDTA. To isolate PBMCs, dextran (6%) was gently added (vol/vol) to the whole blood, and the mixture was incubated at room temperature for 45 min. PBMCs were then isolated from the upper layer of the mixture. Splenocytes were isolated by mechanical disruption from spleens. A similar nonenzymatic approach was used to obtain single-cell suspensions from pancreata. BMMNCs, PBMCs, splenocytes, and tumor cells underwent red blood cell lysis with LCK lysis buffer as described (26). Cells from each preparation were stained with fluorochrome-conjugated CD11b and Gr1 antibodies (BD BioScience). Populations of CD11b+Gr1+ cells were analyzed in each preparation by FACS using a FACS-Calibur instrument (BD BioSciences).

Immunofluorescence and VSA Measurement. Whole pancreata were incubated in sucrose (30%) for 5–10 min at 4°C, followed by washing with PBS (twice 15 min each). Pancreata were then placed in cryomolds containing OCT (Sakura Finetek) medium and were maintained at −70°C. Sections (6 μm) of pancreata were cut from each OCT block by using a cryostat instrument (Leica Microsystems) and maintained at −70°C. Using the Vision Biosystems BOND-maX autostainer, we stained tumor sections with both a hamster anti-CD31 and a rat anti-Gr1 antibodies, respectively, then subsequently stained them with secondary antibodies, including a Cy3 goat anti-hamster (Jackson Immunoresearch) and a rabbit anti-rat 488 (Molecular Probes). Finally, sections were mounted in fluorescent mounting medium (DAKO) containing DAPI (Molecular Probes) for nuclear visualization. Anti-Gr1 and anti-CD11B costaining was carried out in a similar fashion with the fluorophore-conjugated antibodies used for FACS. VSA was measured in each treatment by using CD31 staining, as described, in all identifiable images (≈650 images from all treatments). For VSA measurement, regions of tumors from each section were scanned at ×20 magnification (Applied Imaging Ariol SL-50 Instrument and Review Software), and tumor vasculature was quantified by using algorithm in Metamorph software (Molecular Dynamics).

Statistical analysis. Student's *t* test was applied to all of the analyses, and differences with $P \leq 0.05$ were considered significant.

1. Ferrara N, Kerbel RS (2005) Angiogenesis as a therapeutic target. *Nature* 438:967–974.
2. Ferrara N, Gerber HP, LeCouter J (2003) The biology of VEGF and its receptors. *Nat Med* 9:669–676.
3. Ferrara N, *et al.* (1996) Heterozygous embryonic lethality induced by targeted inactivation of the VEGF gene. *Nature* 380:439–442.
4. Ferrara N, Mass RD, Campa C, Kim R (2007) Targeting VEGF-A to treat cancer and age-related macular degeneration. *Annu Rev Med* 58:491–504.
5. Shojaei F, Ferrara N (2007) Antiangiogenic therapy for cancer: An update. *Cancer J* 13:345–348.
6. Coussens LM, Werb Z (2002) Inflammation and cancer. *Nature* 420:860–867.
7. Shojaei F, *et al.* (2007) Bv8 regulates myeloid cell-dependent tumor angiogenesis *Nature* 450:825–831.
8. Hanahan D, Folkman J (1996) Patterns and emerging mechanisms of the angiogenic switch during tumorigenesis. *Cell* 86:353–364.
9. Bergers G, Javaherian K, Lo KM, Folkman J, Hanahan D (1999) Effects of angiogenesis inhibitors on multistage carcinogenesis in mice. *Science* 284:808–812.
10. Inoue M, Hager JH, Ferrara N, Gerber HP, Hanahan D (2002) VEGF-A has a critical, nonredundant role in angiogenic swithing and pancreatic β cell carcinogenesis. *Cancer Cell* 1:193–202.
11. Nozawa H, Chiu C, Hanahan D (2006) Infiltrating neutrophils mediate the initial angiogenic switch in a mouse model of multistage carcinogenesis. *Proc Natl Acad Sci USA* 103:12493–12498.
12. Boisbouvier J, *et al.* (1998) A structural homologue of colipase in black mamba venom revealed by NMR floating disulphide bridge analysis. *J Mol Biol* 283:205–219.
13. Li M, Bullock CM, Knauer DJ, Ehlert FJ, Zhou QY (2001) Identification of two Prokineticin cDNAs: Recombinant proteins potently contract gestrointestinal smooth muscle. *Mol Pharmacol* 59:692–698.
14. LeCouter J, *et al.* (2001) Identification of an angiogenic mitogen selective for endocrine gland endothelium. *Nature* 412:877–884.
15. LeCouter J, *et al.* (2003) The endocrine-gland-derived VEGF homologue Bv8 promotes angiogenesis in the testis: Localization of Bv8 receptors to endothelial cells. *Proc Natl Acad Sci USA* 100:2685–2690.
16. Kaser A, Winklmayr M, Lepperdinger G, Kreil G (2003) The AVIT protein family. *EMBO Rep* 4:469–473.
17. Masuda Y, *et al.* (2002) Isolation and identification of EG-VEGF/prokineticins as cognate ligands for two orphan G protein-coupled receptors. *Biochem Biophys Res Commun* 293:396–402.
18. Lin DC, *et al.* (2002) Identification and molecular characterization of two closely related G protein-coupled receptors activated by prokineticins/endocrine gland vascular endothelial growth factor. *J Biol Chem* 277:19276–19280.
19. Mollay C, *et al.* (1999) Bv8, a small protein from frog skin and its homologue from snake venom induce hyperalgesia in rats. *Eur J Pharmacol* 374:189–196.
20. Joubert FJ, Strydom DJ (1980) Snake venom: The amino acid sequence of protein A from Dendroaspis polylepis polylepis (black mamba) venom. *Hoppe-Seylers Zeitschrift Physiol Chem* 361:1787–1794.
21. Schweitz H, Pacaud P, Diochot S, Moinier D, Ladzunski M (1999) MIT(1), a black mamba intestinal toxin with a new and highly potent activity on intestinal contraction. *FEBS Lett* 461:183–188.
22. Cheng MY, *et al.* (2002) Prokineticin 2 transmits the behavioral circadian rhythm of the suprachiasmatic nucleus. *Nature* 417:405–410.
23. Ng KL, *et al.* (2005) Dependence of olfactory bulb neurogenesis on prokineticin 2 signaling. *Science* 308:1923–1927.
24. Matsumoto S, *et al.* (2006) Abnormal development of the olfactory bulb and reproductive system in mice lacking prokineticin receptor PKR2. *Proc Natl Acad Sci USA* 103:4140–4145.
25. Dode C, *et al.* (2006) Kallmann syndrome: Mutations in the genes encoding prokineticin-2 and prokineticin receptor-2. *PLoS Genet* 2:e175.
26. LeCouter J, Lin R, Ferrara N (2002) Endocrine gland-derived VEGF and the emerging hypothesis of organ-specific regulation of angiogenesis. *Nat Med* 8:913–917.
27. Lin R, LeCouter J, Kowalski J, Ferrara N (2002) Characterization of EG-VEGF signaling in adrenal cortex capillary endothelial cells. *J Biol Chem* 277:8724–8729.
28. LeCouter J, Zlot C, Tejada M, Peale F, Ferrara N (2004) Bv8 and endocrine gland-derived vascular endothelial growth factor stimulate hematopoiesis and hematopoietic cell mobilization. *Proc Natl Acad Sci USA* 101:16813–16818.
29. Dorsch M, *et al.* (2005) PK1/EG-VEGF induces monocyte differentiation and activation. *J Leukocyte Biol* 78:426–434.
30. Yang L, *et al.* (2004) Expansion of myeloid immune suppressor Gr+CD11b+ cells in tumor-bearing host directly promotes tumor angiogenesis. *Cancer Cell* 6:409–421.
31. De Palma M, *et al.* (2005) Tie2 identifies a hematopoietic lineage of proangiogenic monocytes required for tumor vessel formation and a mesenchymal population of pericyte progenitors. *Cancer Cell* 8:211–226.
32. Shojaei F, *et al.* (2007) Tumor refrectoriness to anti-VEGF treatment is mediated by CD11b+Gr1+ myeloid cells. *Nat Biotechnol* 25:911–920.
33. Casanovas O, Hicklin DJ, Bergers G, Hanahan D (2005) Drug resistance by evasion of antiangiogenic targeting of VEGF signaling in late-stage pancreatic islet tumors. *Cancer Cell* 8:299–309.
34. LeCouter J, *et al.* (2003) Mouse endocrine-gland derived vascular endothelial growth factor: A distinct expression pattern from its human ortholog suggests different roles as a regulator of organ-specific angiogenesis. *Endocrinology* 144:2606–2616.
35. Bergers G, *et al.* (2000) Matrix metalloproteinase-9 triggers the angiogenic switch during carcinogenesis. *Nat Cell Biol* 2:737–744.
36. Liang WC, *et al.* (2006) Cross-species VEGF-blocking antibodies completely inhibit the growth of human tumor xenografts and measure the contribution of stromal VEGF. *J Biol Chem* 281:951–961.